

## DEVELOPMENT OF A BOUNDARY CONDITION WALL FUNCTION FOR PARTICULATE FOULING CFD MODELING

**Sverre G. JOHNSEN<sup>1</sup> and Stein Tore JOHANSEN**

<sup>1</sup> SINTEF Materials and Chemistry, N-7465 Trondheim, NORWAY

### ABSTRACT

Modelling of mass transfer of particles to solid surfaces is a considerable challenge in most industrial processes. Using computational fluid dynamics (CFD) directly on these applications is very challenging and costly due to the grid refinement required to capture the complex physical processes that dominate in the near-wall region. We propose a detailed boundary layer model, which can couple the detailed physics in the wall region with the external flow. This mass-transfer wall function can be applied as a boundary condition for coarse grid CFD models. The detailed boundary layer model incorporates external forces, turbulence and hydrodynamic lift and drag. In addition we include the effects of Brownian diffusion, thermophoresis, XDLVO forces and the inter-particle collisions. The particle deposition flux to the wall is modified with an effective adhesion probability, caused by the adhesive forces and the turbulent shear stress statistics.

### NOMENCLATURE

$A$  Total drift velocity,  $m/s$  .  
 $B$  Total diffusion coefficient,  $m^2/s$  .  
 $C_L$  Lift coefficient, dimensionless.  
 $C_p$  Specific heat capacity,  $J/kg K$  .  
 $d$  Diameter,  $m$  .  
 $f_\tau(T_i) = P(T_i \leq \tau < T_i + dT_i)$  Shear stress probability density function, dimensionless.  
 $\bar{f}$  Force vector per unit volume,  $N/m^3$  .  
 $\bar{F}$  Force vector,  $N$  .  
 $\bar{g}$  Gravity,  $m/s^2$  .  
 $h$  Particle-wall separation,  $m$  .  
 $h_{p,l}$  Particle-liquid heat transfer coefficient,  $W/m^2K$  .  
 $J$  Mass flux,  $kg/m^2s$  .  
 $k_B$  The Boltzmann constant,  $1.3807 \cdot 10^{-23} J/K$  .  
 $k_h$  Thermal conductivity,  $W/mK$  .  
 $m$  Particle mass,  $kg$  .  
 $P$  Pressure,  $Pa$  .  
 $P(X)$  Probability of the event  $X$  , dimensionless.  
 $Pr$  Prandtl number, dimensionless.  
 $q$  Heat flux,  $W/m^2$  .  
 $Sc$  Schmidt number, dimensionless.  
 $t_p$  Particle drag force relaxation time,  $s$  .  
 $T$  Temperature,  $K$  .  
 $u_\tau$  Shear velocity,  $m/s$  .

$\bar{u}$  Liquid velocity vector,  $m/s$  .  
 $\bar{v}$  Particle velocity vector,  $m/s$  .  
 $x$  Cartesian coordinate, parallel to the wall,  $m$  .  
 $y$  Cartesian coordinate, normal to and pointing away from the wall,  $m$  .  
 $\alpha$  Volume fraction, dimensionless.  
 $\beta_\tau$  Thermophoretic force strength, dimensionless.  
 $\mu$  Dynamic viscosity,  $Pa s$  .  
 $\nu$  Kinematic viscosity,  $m^2/s$  .  
 $\rho$  Mass density,  $kg/m^3$  .  
 $\sigma_\tau$  Shear stress standard deviation,  $Pa$  .  
 $\tau_L$  Lagrangian time-scale,  $s$  .  
 $\tau$  Shear stress tensor,  $Pa$  .  
 $\tau, T$  Shear stress,  $Pa$  .

### Subscripts

$bulk$  Value outside the boundary layer.  
 $c$  Critical.  
 $l, p, w$  Property of the liquid, particle, wall.  
 $g, t$  Granular, turbulent contribution.  
 $wall$  Value at the wall.

### Superscripts

$+$  Dimensionless variable.  
 $G$  Granular collisional contribution.  
 $R$  Random contribution.  
 $S$  Soret (thermophoretic) contribution.  
 $T$  Thermal contribution.  
 $XDLVO$  Extended DLVO theory contribution.

### Averaging

$\langle \rangle$  Ensemble average.  
 $"$  Fluctuation about an ensemble averaged value.

### INTRODUCTION

Fouling of solid surfaces exposed to fluids carrying particles is a common and much investigated problem. Fouling is defined as accumulation of unwanted material on solid surfaces. The topic is of general interest in most process industries, including oil/gas, minerals, metals, cement, food, marine and fishing, and also areas like medicine and environment. Consequently, a vast amount of work has been done in this field. Sippola and Nazaroff (2002) and Guha (2008) cite an extensive list of published studies. They give comprehensive reviews of transport and deposition mechanisms for particles in gas and liquid flows, but neither of them includes near-wall XDLVO for-

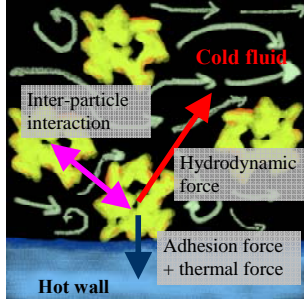


**Figure 1:** Schematic of the flow of a cold suspension at a hot wall. Particles are affected by inter particle interactions, hydrodynamic, thermal and particle-wall forces.

ces or granular stress effects. Johansen (1991a) describes the deposition of particles from a gas flow. Combined thermal-turbulent deposition was, for the first time, predicted by Johansen (1991b) (for gases) and for liquids by Adomeit and Renz (1996).

In a previous paper (Johnsen and Johansen, 2009) we developed a mathematical model for the transport of a dispersed phase, through a turbulent boundary layer, to a solid surface. By numerical solution of the transport equations for the particle volume fraction, temperature and axial mixture velocity, we obtained the particle mass transfer coefficient, which may be employed as a wall boundary value for coarse grid CFD models. The model includes the hydrodynamic forces, drag and lift, thermophoresis, turbulence, granular stress effects and near-wall XDLVO forces, and it is solved on a 1-dimensional grid able to capture the detailed physics close to the wall.

In this paper we modify the calculated particle wall flux by an adhesion probability derived from the turbulent shear stress probability density function. It is assumed that turbulent bursts, above some critical value depending on the adhesive force, may re-entrain deposited particles, reducing the net deposition rate. Several review papers and bibliographies on resuspension of deposited material exist, (e.g. Sehmel, 1980; Nicholson, 1988; Ziskind *et al.*, 1995; Visser, 1995). Re-entrainment/resuspension is defined as the removal of deposited particles from the solid surface, or rebounding of incoming particles, and is the opposite of deposition/fouling.

First, we give a brief overview of the previous model developed (Johnsen and Johansen, 2009). Next we compare results obtained from our model to experimental data on magnetite (Newson *et al.*, 1983) and asphaltene (Jalalialahmadi *et al.*, 2009) deposition.

## GOVERNING EQUATIONS

We consider an Eulerian-Eulerian two-fluid model, consisting of an incompressible continuous liquid ( $l$ ) and a mono-disperse incompressible inert particulate phase ( $p$ ), flowing along a hot wall, as illustrated in Figure 1. For simplicity, we will most of the time omit the  $p$  index when addressing particle properties. Steady turbulent flow is assumed, where the model equations can be derived from volume and ensemble averaged Navier-Stokes equations coupled with heat transport equations. We do not consider thermodynamic effects, so particle generation or phase transitions do not occur.

## Averaging Procedures and Notation

In order to handle the unknown distribution of the constituents inside a given control volume, the conservation equations are derived by volume averaging over the same control volume. The details on volume averaging may be found in classical textbooks on multiphase flow (e.g. Crowe *et al.*, 1997; Soo, 1989). Moreover, the conservation equations are ensemble averaged to account for all possible micro states. All quantities are thus understood as volume and ensemble averages, with no further notice.

Finally, when introducing turbulence, there will be yet another layer of ensemble averaging, to handle the influence on the particles by the stochastic turbulent fluctuations, denoted by  $\overline{\cdot}$ , of the liquid properties.

## Conservation Equations

Without turbulence, the stationary particle phase continuity equation is

$$\overline{\nabla}(\rho_p \alpha_p \bar{\mathbf{v}}) = 0, \quad (1)$$

and the stationary liquid and particulate momentum equations are

$$\overline{\nabla}(\alpha_l \rho_l \bar{\mathbf{u}} \bar{\mathbf{u}}) = - \underbrace{\alpha_l \overline{\nabla P}}_{\text{Pressure gradient}} + \underbrace{\alpha_l \overline{\nabla \boldsymbol{\tau}_l}}_{\text{Viscous stress}} + \underbrace{\alpha_l \rho_l \bar{\mathbf{g}}}_{\text{External fields}} + \underbrace{\bar{\mathbf{f}}_{p,l}}_{\text{Particle-liquid interactions}}, \quad (2)$$

and

$$\overline{\nabla}(\alpha_p \rho_p \bar{\mathbf{v}} \bar{\mathbf{v}}) = - \underbrace{\alpha_p \overline{\nabla P}}_{\text{Pressure gradient}} + \underbrace{\alpha_p \overline{\nabla \boldsymbol{\tau}_l}}_{\text{Viscous stress}} + \underbrace{\alpha_p \rho_p \bar{\mathbf{g}}}_{\text{External fields}} - \underbrace{\bar{\mathbf{f}}_{p,l}}_{\text{Particle-liquid interaction}} + \underbrace{\bar{\mathbf{f}}_p^{XDLVO}}_{\text{Near wall force}}, \quad (3)$$

where the particle -liquid interaction force is given by

$$\bar{\mathbf{f}}_{p,l} = \underbrace{\frac{\alpha_p \rho_p}{t_p} (\bar{\mathbf{v}} - \bar{\mathbf{u}})}_{\text{Drag force}} + \underbrace{\alpha_p \rho_p C_{L,p} (\bar{\mathbf{v}} - \bar{\mathbf{u}}) \times (\overline{\nabla} \times \bar{\mathbf{u}})}_{\text{Lift force}} + \underbrace{\langle \alpha_p \bar{\mathbf{f}}_p^T \rangle}_{\text{Thermal force}}. \quad (4)$$

The brackets enclosing the convective term on the left and the thermal force contribution on the right hand side of Eq. (3) indicate ensemble averages of the entire terms. These terms will be discussed below.

In general there will be a transport of heat between the wall and the bulk. The heat will be transported through the boundary layer by the fluid and the particles. The stationary y-directional heat transport equations for the liquid and particle phases are

$$\underbrace{\frac{\partial(\alpha_l \rho_l C_{p,l} u_y T_l)}{\partial y}}_{\text{Convection}} = \frac{\partial}{\partial y} \left[ \underbrace{\alpha_l k_{h,l}}_{\text{Conduction}} \frac{\partial T_l}{\partial y} \right] + \underbrace{\frac{3\alpha_p h_{p,l}}{4d_p} (T_p - T_l)}_{\text{Particle-liquid heat exchange}}, \quad (5)$$

$$\frac{\partial}{\partial y} \left( \underbrace{\alpha_p \rho_p C_{p,p} v_y T_p}_{\text{Convective heat transport}} - \underbrace{\frac{\alpha_p \rho_p v_g C_{p,p}}{\text{Pr}_{g,p}} \frac{\partial T_p}{\partial y}}_{\text{Collisional heat exchange}} \right) = - \underbrace{\frac{3\alpha_p h_{p,l}}{4d_p} (T_p - T_l)}_{\text{Particle-liquid heat exchange}}, \quad (6)$$

where it is assumed that specific heat capacities,  $C_p$ , are constant, and that the enthalpy may be expressed as  $C_p T$ .

### Momentum contributions

The particles are affected by the viscous stress in the fluid, reflected through the pressure gradient and shear stress contributions. The external field term contains body forces such as gravity and electrostatic forces. We consider vertical flow in the direction of gravity only, and we do not consider electrostatic forces.

The particle-liquid interaction terms are hydrodynamic drag and lift and thermal interactions. Unsteady forces, such as the virtual mass effect or the Basset history term, are not taken into account. The drag force is modelled by Stokes' law,  $t_p = \rho d^2 / 18 \mu_l$ , and the lift force is modelled by the Saffman lift force. Liquid vorticity and particle rotations are neglected, so there is no Magnus lift. The thermal force gives a thermophoretic (Soret) contribution in the presence of temperature gradients, as modelled by McNab and Meisen (1973). In addition, thermally agitated fluid molecules bombarding the particles generate thermal particle velocities entering through the left-hand-side convective term of Eq. (3).

The short-ranged particle-wall interaction is modelled by the extended DLVO theory (XDLVO), including the Lifshitz-van der Waals, electrostatic double-layer, and acid-base forces, based on the model developments of Hoek and Agarwal (2006) and van Oss (2006). The XDLVO model is derived for a perfectly smooth particle close to a perfectly smooth surface. Thus, depending on the particle and wall roughness, the XDLVO theory is not directly applicable to large particles. As was shown in a previous paper (Johnsen and Johansen, 2009), however, the large-particle deposition flux is not very sensitive to the XDLVO contribution, so no upper particle size limit has been imposed.

### The Convective Term

We consider the particle velocity on three different scales; macro (average particle velocity), meso (granular stress), and micro (thermal stress). The source of the granular stress is the particle-particle collisions that occur in dense suspensions, while the thermal stress is due to collisions between the particles and thermally agitated fluid molecules. By adopting the simplifying assumption that there is no correlation between the scales, the left-hand-side convective term of Eq. (3) becomes

$$\bar{\nabla} \langle \alpha \rho \bar{\mathbf{v}} \bar{\mathbf{v}} \rangle \rightarrow \bar{\nabla} \left\{ \alpha \rho \langle \bar{\mathbf{v}} \rangle \langle \bar{\mathbf{v}} \rangle + \langle \alpha \rho \bar{\mathbf{v}}^{-G} \bar{\mathbf{v}}^{-G} \rangle + \langle \alpha \rho \bar{\mathbf{v}}^{-T} \bar{\mathbf{v}}^{-T} \rangle \right\}, \quad (7)$$

where  $\langle \bar{\mathbf{v}} \rangle$  is the ensemble averaged velocity vector, and  $\bar{\mathbf{v}}^{-G}$  and  $\bar{\mathbf{v}}^{-T}$  contain the deviatory components caused by particle collisions and thermal fluctuations, respectively. The granular stress gives a non-Newtonian contribution to the particle-liquid mixture viscosity and a pressure contribution preventing too high particle concentrations. The thermal stress gives the Brownian diffusivity.

### Turbulence modelling

The liquid velocity consists of an average and a fluctuating part due to turbulence,  $\bar{\mathbf{u}} = \langle \bar{\mathbf{u}} \rangle + \bar{\mathbf{u}}''$ . We employ the turbulence model, for the kinematic eddy

viscosity,  $\nu_{t,l}$ , and the fluid rms velocity,  $u_y^{n+}$ , of Johansen (1991a).

Assuming that the probability density function (pdf) of the liquid velocity is the Gaussian normal distribution,  $N(\langle \bar{\mathbf{u}} \rangle, \sigma_u^2)$ , it can be shown that the liquid shear-stress is also given by a normal distribution,  $N(\langle \tau_{l,wall} \rangle, \sigma_\tau^2)$ , where  $\sigma_\tau = \langle \tau_{l,wall} \rangle \sqrt{(u_x^{n+})^2 + (u_z^{n+})^2}$ . Utilizing the liquid velocity rms values given by Kim *et al.* (1987), we get  $\sigma_\tau \approx 0.404 \langle \tau_{l,wall} \rangle$ , so that the pdf of the shear stress is given by

$$f_\tau(T_l) = \frac{1}{0.404 \sqrt{2\pi} \langle \tau_{l,wall} \rangle} \exp \left[ -\frac{(T_l - \langle \tau_{l,wall} \rangle)^2}{0.326 \langle \tau_{l,wall} \rangle^2} \right]. \quad (8)$$

### NEAR-WALL MODEL

Close to the wall, the flow regime is radically different from that of the bulk, and we may, because of this, impose several simplifying assumptions on the governing equations, in addition to those already mentioned. We will assume a boundary layer situation where there are two principal directions,  $x$  (parallel to the wall) and  $y$  (normal to and pointing away from the wall, into the liquid). We limit the study to low particle deposition rates, so it will be assumed that axial gradients are negligible, such that  $\partial/\partial x = 0$ , for all quantities. We furthermore assume that the particle velocity normal to the wall is negligible outside the boundary layer, at  $y = y_{bulk} \gg d/2$ , and we get, by integrating Eq. (1) from  $y = d/2$  to  $y_{bulk}$ , the stationary particle deposition flux;

$$\frac{J_{y,wall}}{y_{bulk}} \approx -\frac{\partial}{\partial y} (\rho \alpha v_y). \quad (9)$$

Moreover, we assume that the liquid velocity normal to the wall is negligible within the boundary layer.

Adding up the axial components of the momentum equations, Eqs. (2) and (3), averaging over turbulent fluctuations, neglecting the inertial terms and assuming that the  $x$ -directional particle and liquid velocities only differ by a constant terminal velocity, we get the axial mixture momentum equation,

$$1 = \left[ 1 + \frac{v_t^+ \rho_{mix}}{\rho_l} + \frac{\mu^G}{\mu_l} \right] \frac{\partial u_x^+}{\partial y^+}, \quad (10)$$

where we have introduced the dimensionless velocity,  $u_x^+ = u_x / u_\tau$ , distance,  $y^+ = (y - d/2) u_\tau / \nu_l$ , and turbulent kinematic viscosity,  $\nu_t^+ = \nu_t / \nu_l$ . The mixture density is defined as  $\rho_{mix} \equiv \alpha \rho + \alpha_l \rho_l$ , and we have assumed that the particle turbulent viscosity can be approximated by the liquid turbulent viscosity. The granular viscosity gives a non-Newtonian effect when the shear field makes the particles rub against each other.

The normal-to-wall particle velocity may be explicitly obtained from the  $y$  component of Eq. (3) and

expressed as the sum of a convective drift velocity and a diffusive velocity;

$$v_y^+ \Gamma = A^+ - \frac{B^+}{\alpha^+} \frac{\partial \alpha^+}{\partial y^+}, \quad (11)$$

where we have ensemble averaged over turbulent realizations, and  $\Gamma = 1 + (t_p^+ / \alpha^+ v_y^+) \partial (\alpha^+ (v_y^+)^2) / \partial y^+$ . For stability reasons, we approximate  $\Gamma \approx 1$ , which is appropriate except in the XDLVO-dominated sub-layer close to the wall. The effective convective drift velocity is given by

$$A^+ = t_p^+ \left[ \underbrace{\frac{1}{t_p^+} \frac{\beta_T}{T^+ + T_0^+} \frac{\partial T^+}{\partial y^+}}_{\text{Thermophoresis}} - \underbrace{\frac{\tau_L^+}{\tau_L^+ + t_p^+} \frac{\partial \langle (u_y^+)^2 \rangle}{\partial y^+}}_{\text{Turbophoresis}} \right. \\ \left. + \underbrace{\frac{3.08 \mu_l}{u_\tau \rho d_p} \sqrt{\frac{\partial u_x^+}{\partial y^+}} (v_x^+ - u_x^+)}_{\text{Hydrodynamic lift}} + \underbrace{F_y^{\text{XDLVO}^+}}_{\text{XDLVO forces}} - \underbrace{\frac{\partial P^{G^+}}{\partial y^+}}_{\text{Granular pressure}} \right], \quad (12)$$

and the effective diffusivity is expressed as

$$B^+ = t_p^+ \left[ \underbrace{\frac{k_B q_{\text{wall}}}{\rho_l u_\tau^3 m_p C_{p,l}} (T^+ + T_0^+)}_{\text{Brownian diffusivity}} + \underbrace{\frac{\langle (u_y^+)^2 \rangle \tau_L^+}{\tau_L^+ + t_p^+}}_{\text{Turbophoretic diffusivity}} + \underbrace{\frac{1}{t_p^+ (1 - \alpha)} \frac{v_l^+}{Sc_i}}_{\text{Turbulent diffusivity}} \right], \quad (13)$$

and we have introduced several dimensionless parameters and variables;  $\alpha^+ = \alpha / \alpha_{\text{bulk}}$ ,  $t_p^+ = t_p u_\tau^2 / \nu_l$ ,  $\rho_l^+ = \rho_l / \rho$ ,  $T^+ = (T_l - T_{\text{wall}}) u_\tau \rho_l C_{p,l} / q_{\text{wall}}$ ,  $T_0^+ = u_\tau \rho_l C_{p,l} T_{\text{wall}} / q_{\text{wall}}$ ,  $P^{G^+} = P^G / \rho \alpha_{\text{bulk}} u_\tau^2$ , and  $F_y^{\text{XDLVO}^+} = F_y^{\text{XDLVO}} 6 \nu_l / \pi d_p^3 \rho u_\tau^3$ . Combining Eqs. (9) and (11) we may express the dimensionless wall flux,  $J_{\text{wall}}^+ = J_{\text{wall}} / u_\tau \rho \alpha_{\text{bulk}}$ , as

$$-\frac{J_{\text{wall}}^+}{y_{\text{bulk}}^+} = \frac{\partial}{\partial y^+} \left[ \Gamma^{-1} \alpha^+ A^+ - \Gamma^{-1} B^+ \frac{\partial \alpha^+}{\partial y^+} \right]. \quad (14)$$

Introducing turbulence, ensemble averaging and adding the two energy equations Eqs. (5) and (6) and assuming identical particle and liquid temperatures, we get

$$-\text{Pr} = \left[ 1 + k_h^{G^+} + k_{h,t,l}^+ + k_{h,t,p}^+ \right] \frac{\partial T^+}{\partial y^+}, \quad (15)$$

where the dimensionless thermal conductivities are defined as  $k_h^+ = k_h / k_{h,l}$ . We let the turbulent liquid and particle thermal conductivities be defined as  $k_{h,t,l} \equiv C_{p,l} \alpha_l \rho_l \nu_{l,l} / \text{Pr}_{l,l}$ , and  $k_{h,t,p} \equiv C_{p,p} \alpha_p \rho_p \nu_{l,p} / \text{Pr}_{l,p}$ , and we define the granular heat conductivity as  $k_h^G \equiv -\alpha k_{h,l} - C_{p,p} \alpha_p \nu_y T + C_{p,p} \alpha_p \nu_g / \text{Pr}_{g,p}$ . The turbulent liquid heat conductivity improves the liquid heat transport because of the mixing processes generated by the turbulent fluctuations. The overall heat conductivity is

modified by the presence of the particle phase, and these effects are represented by the granular and turbulent particle heat conductivities. The granular heat conductivity contains a reduction in the liquid heat conductivity due to the reduced liquid volume fraction, a convective particle heat transport contribution, and a contribution accounting for heat exchange between colliding particles. For low deposition rates, it is reasonable to neglect the convective particle heat transport. The turbulent particle heat conductivity accounts for the additional heat transport by turbulent particle fluctuations.

### Adhesion Probability

Due to the turbulent fluctuations of the shear stress given by the pdf in Eq. (8), deposited particles may detach and inbound particles may not stick. It is assumed that wall shear stresses larger, in magnitude, than some critical wall shear stress,  $T_{l,c}$ , result in re-entrainment. Even if the average wall shear stress is below the critical value, turbulent bursts may momentarily generate shear stresses above the critical value. At the critical shear stress, the shear force acting on the projected area of a particle cancels out the adhesive force,  $\pi d^2 T_{l,c} / 4 = F_{\text{adhesion}}$  (Johansen, 1991b). Integrating Eq. (8), the probability of adhesion thus becomes

$$P_{\text{adhesion}} = P(-T_{l,c} < \tau_l < T_{l,c}) = \int_{-T_{l,c}}^{T_{l,c}} f_\tau(T_l) dT_l \\ = \frac{1}{2} \left[ \text{erf} \left( \frac{T_{l,c} - \langle \tau_{l,\text{wall}} \rangle}{0.571 \langle \tau_{l,\text{wall}} \rangle} \right) - \text{erf} \left( \frac{-T_{l,c} - \langle \tau_{l,\text{wall}} \rangle}{0.571 \langle \tau_{l,\text{wall}} \rangle} \right) \right], \quad (16)$$

where  $\text{erf}(\dots)$  is the Gauss error function. To account for the reduced deposition flux, due to shear stress induced re-entrainment, we increase the fouling resistance by multiplying the rhs of Eq. (14) by the adhesion probability of Eq. (16).

### Adhesive Forces

When a particle is residing at the wall, the sum of forces acting on the particle will determine if the particle sticks or not. A net force acting towards the wall will make the particle adhere, while a net force pointing away from the wall will re-entrain the particle. We define the adhesive force as being the sum of the XDLVO, the thermophoretic, and the Saffman lift forces, calculated at the  $j=1$  grid cell,

$$F_{\text{adhesion}} = \left[ F_y^{\text{XDLVO}} + F_y^{\text{Soret}} + F_y^{\text{Saff}} \right]_{y_1}. \quad (17)$$

In addition, the particle is subject to hydrodynamic drag/shear stress, as discussed above.

The adhesive force strongly depends on the particle-wall minimum separation distance, since the Lifshitz-van der Waals contribution diverges as the separation goes to zero. Accepting too small particle-wall separation distances, in the model, result in extremely strong adhesive forces, making re-entrainment impossible. In reality, surface roughness will give a particle-size dependent minimum particle-wall separation, reducing the adhesive force acting on large particles. Reduced adhesive

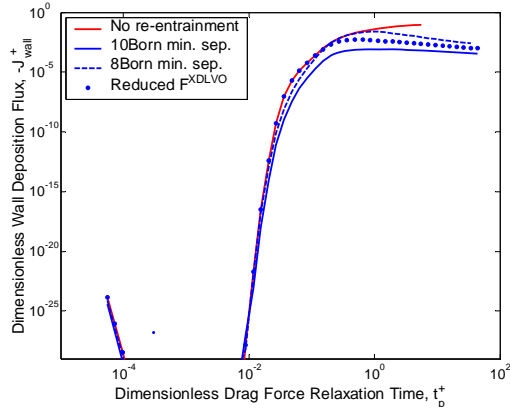


**Figure 2:** The dimensionless wall-flux as a function of dimensionless particle relaxation time. Large diameters correspond to large  $t_p^+$ . Comparison of a non-re-entrainment model (red) and models featuring adhesion probability correction to the wall flux (blue). Re-entrainment is obtained by reducing the adhesive force by increasing the minimum particle-wall separation or by applying a reduction factor to the XDLVO force.

forces may be obtained by applying a correction factor to the XDLVO force and/or increasing the minimum particle-wall separation. Biasi *et al.* (2001) suggested a particle size dependent correction factor to account for the effect of surface roughness,

$$\frac{F_{adhesion}}{F_y^{XDLVO}} \Big|_{wall} = 0.016 \left[ 1 - 0.1d^{0.545} \right]. \quad (18)$$

As is seen in Figure 2, we get a similar re-entrainment effect on the deposition rate, when increasing the minimum particle-wall separation. The Figure 2 data are based on the calcium carbonate-water system described in Johnsen and Johansen (2009), including all interaction terms.

## NUMERICAL SOLUTION ALGORITHM

The system of equations, Eq. (10), Eq. (14) and Eq. (15), are solved numerically, for  $u_x^+$ ,  $\alpha^+$  and  $T^+$ , on a discrete grid, which extends from  $y_1 = d/2 + h_{min}$  to  $y_{1000} = 0.01m$ , where  $h_{min}$  is the minimum particle-wall separation. The grid point distances,  $y_j - y_{j-1}$ , increase logarithmically, and cell interfaces are put half-way between neighbouring grid points. Refer to Johnsen and Johansen (2009) for details on the numerical algorithm and the boundary conditions.

## RESULTS AND DISCUSSION

In Johnsen and Johansen (2009) the effects of the various physical phenomena, including turbulence, thermophoresis, granular pressure and XDLVO near-wall forces were explored, and the way particles of different diameters experience the various forces, by applying the model to a steel surface-calcium carbonate-water system, was studied. It was assumed that the wall was a perfect sink, so that all particles arriving at the wall were deposited. It was seen that particles of different size may

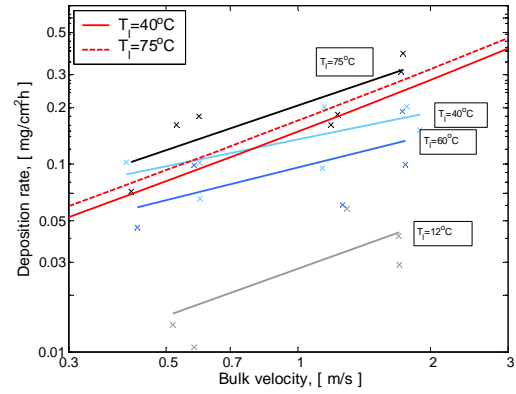


**Figure 3:** Comparison of modelled deposition rates (red) and experimental deposition rates, with linear best-fit curves, in a dilute suspension of magnetite and water (Newson *et al.*, 1983), at different temperatures.

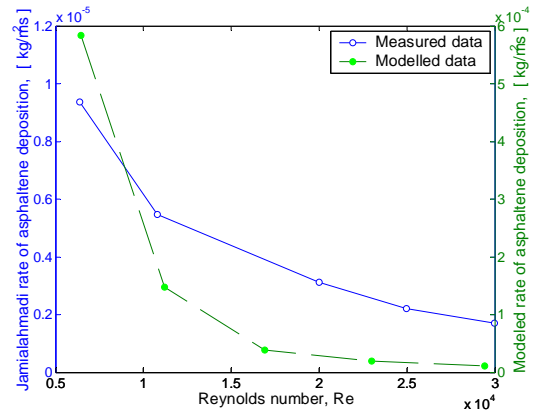


**Figure 4:** Comparison of modelled and measured asphaltene deposition rates (Jamialahmadi *et al.*, 2009), for different Reynolds numbers (flow velocities).

experience very different transport mechanisms, and that very low deposition rates are expected for particles smaller than  $3 \mu m$ .

In this paper we have strengthened the model by including re-entrainment of deposited particles by turbulent bursts. We demonstrate how the particle deposition rate is affected by allowing for re-entrainment, by modifying the particle wall flux by a shear stress dependent adhesion probability. The deposition rate will, in general, increase for increasing velocities until the shear induced re-entrainment rate becomes of the same order as the deposition rate. Thereafter the deposition rate will decrease for increasing velocities. Large particles are generally more easily re-entrained than small particles because of the weaker adhesive force and because they cannot easily hide in the viscous sub-layer. As is seen in Figure 2, the effect of re-entrainment becomes important for particles of about  $t_p^+ = 5 \cdot 10^{-2}$ . Particle sizes 1 and  $5 \mu m$  correspond to  $t_p^+ = 5.5 \cdot 10^{-3}$  and  $1.4 \cdot 10^{-1}$ , respectively.

Our model predicts reasonably well, with no parameter fitting, the deposition rate data reported by Newson *et al.* (1983), for a dilute magnetite-water suspension flowing in an aluminium pipe, as is shown in

Figure 3. Newson reports no XDLVO parameters, and there was no reported temperature gradient in the system, so the XDLVO and thermophoretic forces were left out, and the magnetite concentration was too low to produce any granular stress effects, leaving us with Brownian motion, lift and turbulence. The Newson data show significant scatter, but the linear best-fit curves show the same tendency of increasing deposition rates for increasing bulk velocities, as the model. The model yields increasing deposition rates for increasing temperatures, due to the strengthened Brownian motion, although the effect looks smaller than seen from the Newson data. It should also be noted that the Newson deposition rates are not monotonously increasing for increasing temperature.

Shrinking deposition rates for increasing bulk velocities was demonstrated in the asphaltene deposition experiments performed by Jamalhamadi *et al.* (2009). They studied the asphaltene deposition rates of an Iranian asphaltenic crude oil flowing through a stainless steel pipe. No XDLVO parameters or thermophoretic strength is reported for the asphaltene particles, and it is evident from the experimental data that thermodynamics give significant contributions. Crude oil systems are complex thermo-chemical systems, and asphaltene deposition is an extremely complex problem. Our model does not incorporate thermodynamic effects, and both the XDLVO parameters and the thermophoresis are expected to give crucial contributions to the particle transport and adhesion, so it is no surprise that our model cannot, straight away, predict the numerical value of the deposition rates. As is shown in Figure 4, however, the model reproduced the reduced deposition rate trend as the bulk velocity increases. In order to make the model predict more accurately the experimental data, measurement of the input parameters is needed and the model is in need of further development to handle thermo-chemical behaviour.

## CONCLUSIONS

A one-dimensional model has been developed for particle transport and deposition, in the turbulent boundary-layer, including Brownian diffusion, thermophoresis, XDLVO near-wall forces, granular stress and shear induced re-entrainment. It has been seen that re-entrainment can reduce the deposition rate of large particles significantly. The model can be employed to calculate mass-transfer coefficients for the particle phase, and may hence be implemented as a mass transfer boundary wall-function for coarse grid CFD simulations. Results obtained from the model were compared to experimental results on magnetite and asphaltene deposition. Due to lack of detailed model input, the model could not accurately predict the experimental data, but the trend of flow velocity dependency of the deposition rate was reproduced. The model is in need of thermo-chemical capabilities to handle complex deposition phenomena.

## ACKNOWLEDGMENTS

This work was a part of the FOULSURFACE project which was carried out in MATERA ERA-Net cooperation between VTT Technical Research Centre of Finland, University of Oulu, SINTEF and University College Dublin. The project is jointly funded by Tekes, The Research Council of Norway, Enterprise Ireland, VTT, SINTEF and seven industrial companies from Finland,

Sweden and Austria. The authors thank the research partners and funding organizations.

## REFERENCES

- ADOMEIT, P. and RENZ, U., (1996), "Deposition of Fine Particles from a Turbulent Liquid Flow: Experiments and Numerical Predictions", *Chem. Eng. Sci.*, **51**, 3491-3503.
- BIASI, L. *et al.*, (2001), "Use of a Simple Model for the Interpretation of Experimental Data on Particle Resuspension in Turbulent Flows", *J. Aerosol Sci.*, **32**, 1175-1200.
- CROWE, C. *et al.*, (1997), "Multiphase flows with droplets and particles", CRC Press, Boca Raton, Florida, USA.
- GUHA, A., 2008, "Transport and Deposition of Particles in Turbulent and Laminar Flow", *Annular Rev. Fluid Mech.*, **40**, 311-341.
- HOEK, E.M.V. and AGARWAL, G.K., (2006), "Extended DLVO interactions between spherical particles and rough surfaces", *J. Colloid and Interface Sci.*, **298**, 50-58.
- JAMIALAHMADI, M. *et al.*, (2009), "Measurement and Prediction of the Rate of Deposition of Flocculated Asphaltene Particles from Oil", *Intl. J. Heat and Mass Transfer*, in press.
- JOHANSEN, S.T., (1991a), "The Deposition of Particles on Vertical Walls", *Intl. J. of Multiphase Flow*, **17**, 355-376.
- JOHANSEN, S.T., (1991b), "Thermal inertial deposition of particles", *Proc. Intl. Conf. of Multiphase Flows '91 Tsukuba*, **1**, 415-421.
- JOHANSEN, S.G. and JOHANSEN, S.T., (2009), "Deposition Modelling from Multi-Phase Dispersed Flow – A Boundary Layer Wall Function Approach", *Heat Exchanger Fouling and Cleaning – 2009*, Schladming, Austria.
- KIM, J. *et al.*, (1987), "Turbulence Statistics in Fully Developed Channel Flow at Low Reynolds Number", *J. Fluid Mech.*, **177**, 133-166.
- MCNAB, G.S. and MEISEN, A., (1973), "Thermophoresis in Liquids", *J. of Colloid and Interface Science*, **44**.
- NICHOLSON, K.W., (1988), "A Review of Particle Resuspension", *Atm. Env.*, **22**, 2639-2651.
- NEWSON, I.H. *et al.*, (1983), "Studies of Magnetite Deposition from a Flowing Suspension", *Chem. Eng. Commun.*, **20**, 335-353.
- SEHMEL, G.A., (1980), "Particle Resuspension: A Review", *Env. Intl.*, **4**, 107-127.
- SIPPOLA M.R. and NAZAROFF, W.W., (2002), "Particle deposition from turbulent flow: Review of published research and its applicability to ventilation ducts in commercial buildings". Lawrence Berkeley National Laboratory, LBNL-(51432), Berkeley, CA.
- SOO, S.L., (1989), "Particulates and continuum: multiphase fluid dynamics", Hemisphere Publishing Corporation, New York, USA.
- van OSS, C.J., (2006), "Interfacial forces in aqueous media", CRC Press, Boca Raton, Florida, USA.
- VISSER, J., (1995), "Particle Adhesion and Removal: A Review", *Particulate Sci. and Tech.*, **13**, 169-196.
- ZISKIND, G. *et al.*, (1995), "Resuspension of Particulates from Surfaces to Turbulent Flows – Review and Analysis", *J. Aerosol Sci.*, **26**, 613-644.